Clinical features, diagnosis, and survival analysis of dogs with glioma

Affordable 1.5T MRI?
It's within reach.

A revolutionary MRI
built specifically for animals...

Learn more at info.hallmarq.net/jvim-affordable-mri

Hallmarq
Advanced Veterinary Imaging

2021

20 YEARS
2001 - 2021

Received: 25 October 2020 | Accepted: 27 May 2021

DOI: 10.1111/jvim.16199

STANDARD ARTICLE

Journal of Veterinary Internal Medicine Open Access

ACVIM American College of Veterinary Internal Medicine

Clinical features, diagnosis, and survival analysis of dogs with glioma

Roberto José-López[1,2] | Rodrigo Gutierrez-Quintana[1] | Cristian de la Fuente[2] | Edgar G. Manzanilla[3,4] | Anna Suñol[5] | Dolors Pi Castro[2,6] | Sonia Añor[2] | Daniel Sánchez-Masian[7] | Francisco Fernández-Flores[7] | Emanuele Ricci[7] | Katia Marioni-Henry[8] | Joan Mascort[5] | Lara A. Matiasek[9] | Kaspar Matiasek[10] | Paul M. Brennan[11] | Martí Pumarola[2,6]

[1]School of Veterinary Medicine, College of Medical, Veterinary and Life Sciences, University of Glasgow, Glasgow, UK

[2]Department of Animal Medicine and Surgery, Veterinary Faculty, Universitat Autònoma de Barcelona, Barcelona, Spain

[3]School of Veterinary Medicine, University College Dublin, Dublin, Ireland

[4]TEAGASC, The Irish Food and Agriculture Authority, Cork, Ireland

[5]ARS Veterinaria, Barcelona, Spain

[6]Networking Research Center on Bioengineering, Biomaterials and Nanomedicine (CIBER-BBN), Universitat Autònoma de Barcelona, Barcelona, Spain

[7]Institute of Veterinary Science, University of Liverpool, Neston, UK

[8]Royal (Dick) School of Veterinary Studies and Roslin Institute, University of Edinburgh, Edinburgh, UK

[9]Tierklinik Haar, Haar, Germany

[10]Centre for Clinical Veterinary Medicine, Ludwig-Maximilians-Universitaet, Munich, Germany

[11]Translational Neurosurgery, Centre for Clinical Brain Sciences, University of Edinburgh, Edinburgh, UK

Correspondence
Roberto José-López, School of Veterinary Medicine, University of Glasgow, Bearsden Road, Glasgow, G61 1QH, UK.
Email: roberto.jose-lopez@glasgow.ac.uk

Present address
Anna Suñol, Royal (Dick) School of Veterinary Studies, University of Edinburgh, Edinburgh, UK

Dolors Pi Castro, Anicura Arvivet Hospital Veterinari, Barcelona, Spain

Daniel Sánchez-Masian, Anderson Moores Veterinary Specialists, Winchester, UK

Lara A. Matiasek, Anicura Small Animal Clinic, Babenhausen, Germany

Abstract

Background: Gliomas in dogs remain poorly understood.

Objectives: To characterize the clinicopathologic findings, diagnostic imaging features and survival of a large sample of dogs with glioma using the Comparative Brain Tumor Consortium diagnostic classification.

Animals: Ninety-one dogs with histopathological diagnosis of glioma.

Methods: Multicentric retrospective case series. Signalment, clinicopathologic findings, diagnostic imaging characteristics, treatment, and outcome were used. Tumors were reclassified according to the new canine glioma diagnostic scheme.

Results: No associations were found between clinicopathologic findings or survival and tumor type or grade. However, definitive treatments provided significantly ($P = .03$) improved median survival time (84 days; 95% confidence interval [CI], 45-190)

Abbreviations: CBTC, Comparative Brain Tumor Consortium; CE, contrast enhancement; CI, confidence interval; CNS, central nervous system; CSF, cerebrospinal fluid; CT, computed tomography; FLAIR, fluid-attenuation inversion recovery; GFAP, glial fibrillary acidic protein; GRE, gradient-recalled echo; HA, high-grade astrocytoma; HO, high-grade oligodendroglioma; HU, high-grade undefined glioma; LA, low-grade astrocytoma; LO, low-grade oligodendroglioma; MRI, magnetic resonance imaging; MST, median survival time; OR, odds ratio; WHO, World Health Organization.

Funding information
University of Glasgow, Small Animal Hospital Fund Postgraduate Research Grant, Grant/Award Number: 145973-02

compared to palliative treatment (26 days; 95% CI, 11-54). On magnetic resonance imaging (MRI), oligodendrogliomas were associated with smooth margins and T1-weighted hypointensity compared to astrocytomas (odds ratio [OR], 42.5; 95% CI, 2.42-744.97; $P = .04$; OR, 45.5; 95% CI, 5.78-333.33; $P < .001$, respectively) and undefined gliomas (OR, 84; 95% CI, 3.43-999.99; $P = .02$; OR, 32.3; 95% CI, 2.51-500.00; $P = .008$, respectively) and were more commonly in contact with the ventricles than astrocytomas (OR, 7.47; 95% CI, 1.03-53.95; $P = .049$). Tumor spread to neighboring brain structures was associated with high-grade glioma (OR, 6.02; 95% CI, 1.06-34.48; $P = .04$).

Conclusions and Clinical Importance: Dogs with gliomas have poor outcomes, but risk factors identified in survival analysis inform prognosis and the newly identified MRI characteristics could refine diagnosis of tumor type and grade.

KEYWORDS
astrocytoma, dog, magnetic resonance imaging, oligodendroglioma, prognosis, tumor grade, undefined glioma

1 | INTRODUCTION

The incidence of brain tumors in adult dogs is 2.8% to 4.5% and, although individual studies vary, gliomas represent 36% to 70% of primary brain tumors in dogs.[1-5] Consequently, glioma in dogs is increasingly recognized as a naturally occurring model for understanding human glioma. The benefits include the size and structure of the canine brain, the incidence of spontaneous gliomas, and the coexistence with an active immune system.[6,7] Nevertheless, there are many gaps in knowledge related to the natural biology of glioma in dogs as well as its molecular characteristics.

Epidemiologic data on glioma in dogs indicates a median age at diagnosis of 8 years, a male predilection (incidence ratio of 1.53 for males/females), and predominant lesion location within the frontoolfactory, temporal, and parietal lobes of the brain.[3,5,8] Over 50% of all gliomas in dogs occur in certain brachycephalic breeds[3,5,8-10] and the Boston Terrier, Bulldog, and Boxer breeds have a higher prevalence of oligodendroglioma.[8] On magnetic resonance imaging (MRI), intracranial gliomas in dogs are typically described as intra-axial, T1-weighted iso- to hypointense and T2-weighted iso- to hyperintense mass lesions with varying degrees of contrast enhancement (CE).[5,11-14] Oligodendrogliomas are reported to contact the brain surface more commonly, whereas astrocytomas have been associated with more peritumoral edema, lack of ventricular distortion, and iso- to hyperintense T1-weighted signal.[13,14] Tumors with mild to no CE, absent cystic structures, and tumor location other than the thalamocapsular region have been associated with low-grade gliomas.[14] Grade and type of histologically confirmed intracranial gliomas in dogs using these MRI features found an accuracy of 53.3% and 60% for predicted tumor grade and type, respectively.[15]

Standard veterinary practice in recent years has been to use the 2007 World Health Organization (WHO) human glioma classification to grade canine gliomas.[16,17] This classified and graded human tumors based on analysis of clinical outcome and survival relative to specific pathologic criteria. However, little is known about whether histologic tumor type and grade correlates with biologic behavior in canine gliomas. To date, information on tumor progression and outcome after treatment is anecdotal.[18] Since 2007, advances in molecular genetics and biology have enhanced our understanding and subclassification of human gliomas, which led in 2016 to an updated edition of the WHO brain tumor classification.[19] Subsequently, the Comparative Brain Tumor Consortium (CBTC) of the National Cancer Institute proposed a revised diagnostic classification of canine gliomas.[8] Their aim was to provide an updated canine-specific scheme for clinical and molecular data to be added into a morphologic diagnosis, to assist with prediction of tumor behavior.

The aims of this study were to enhance this revised diagnostic classification by further characterizing the epidemiologic, clinicopathologic, diagnostic imaging, and outcome features of gliomas in dogs in a large sample. We assess the relationship between these features and tumor histological type and grade, based on the new diagnostic classification for dogs.

2 | MATERIALS AND METHODS

This study was approved by the Research Ethics Committee of the School of Veterinary Medicine of the University of Glasgow (Ref33a/17). The clinical records of dogs presented to 7 European referral centers between 2005 and 2018 were retrospectively analyzed. Dogs were included if they had a histopathologic diagnosis of glioma. Samples were obtained by means of surgical biopsy or at necropsy within 24 hours from death.

2.1 | Morphologic diagnosis

All samples were fixed in 10% neutral buffered formalin. Fixation times varied because of the multicentric and retrospective nature of the study;

however, this was always <5 days. After fixation, transverse sections of the brain or spinal cord were made and samples including the tumor area were routinely processed. Morphologic evaluation was performed on 4 μm paraffin-embedded sections stained with hematoxylin and eosin.

All gliomas were reviewed and classified by a board-certified pathologist (M. Pumarola) using the CBTC diagnostic scheme.[8] When available, samples were further evaluated by immunohistochemistry for glial fibrillary acidic protein (GFAP) (Z0334; Dako; Glostrup; Denmark; 30-minute incubation at a dilution of 1:500), and Olig2 protein (AB 9610; Merck Millipore; Darmstadt; Germany; 30-minute incubation at a dilution of 1:100). For both markers, slides were scored on a scale of 0 to 4 as previously described.[20] Immunohistochemical characterization of 16 cases (dogs 10-20, 76-80; Supplementary Table 1) was reported previously.[20-22]

Histopathology reports and available tissue were reviewed for features of infiltrative spread consisting of invasion of adjacent central nervous system (CNS) regions as well as presence of secondary structures of Scherer, including perineuronal and perivascular satellitosis, subpial and subependymal tumor cell condensation, and invasion along white matter tracts.[8,17,19,23] Extension through the corpus callosum into the contralateral hemisphere was documented as butterfly glioma.[19,24] Gliomatosis cerebri growth pattern was recorded as recently defined.[19,25]

Evidence of extension into the subarachnoid space (tumor spread through the pia mater with or without proliferation within the leptomeninges), ventricular invasion or drop metastases was noted.[26-29] Penetration of the bone[21] or infiltration of other non-CNS structures were also recorded. Finally, postmortem examination reports were reviewed for the presence of metastases elsewhere in the body.[5]

2.2 | Anatomic location of tumors

Gliomas were allocated into 1 of 4 main anatomic locations: hemispheric (cerebral hemispheres including deep gray matter), diencephalon, infratentorial, and spinal cord. Within these regions, the specific location of the largest portion of the tumor was recorded as frontoolfactory, parietal lobe (including the adjacent corpus callosum), temporal lobe (including the piriform lobe), occipital lobe, ventricles, diencephalon, cerebellum, brainstem, and spinal cord segment corresponding with the overlying vertebrae.[8,14,30] Furthermore, any degree of involvement of the diencephalon was noted.[5,13]

2.3 | Dog demographics, clinicopathologic data, and staging

Demographic data (age, sex, and breed), presenting clinical signs, and physical and neurologic examination findings were recorded for each case. Clinical signs were annotated as summarized on Table 1.

Cerebrospinal fluid (CSF) analysis results, when available before treatment, were noted.

Reports of cases that underwent diagnostic imaging of the thorax, abdomen, or both for staging were reviewed for the presence of metastases.[5]

2.4 | Magnetic resonance imaging

Magnetic resonance imaging studies were performed with scanners of variable field strength (0.2-1.5 T). All studies included T2-weighted sagittal and transverse sequences and both, precontrast and postcontrast (gadopentate dimeglumine; Magnevist, Bayer Schering Pharma AG, Berlin, Germany) T1-weighted transverse sequences. When available, additional fluid-attenuation inversion recovery (FLAIR) dorsal or transverse sequences, gradient-recalled echo (GRE) transverse sequences, T2-weighted dorsal views, and precontrast and postcontrast T1-weighted dorsal and sagittal views were evaluated.

Magnetic resonance imaging features were independently evaluated by 2 board-certified neurologists (R. Gutierrez-Quintana, R. José-López) and classified based on the consensus opinion. Both observers were aware that lesions were gliomas but were blinded to the histopathologic type and grade and provided with standardized grading instructions. The MRIs were classified on the basis of 20 criteria adapted from a recent study.[14] For each criterion, observers chose 1 option from those specified in Table 2. Spinal cord located gliomas were excluded from the analysis.

Observers were provided with specific instructions for some MRI criteria. If the tumor margins were clear, they were divided into smooth and irregular whereas if they were indistinct, they were considered poorly defined. Each glioma was classified on the basis of signal intensity relative to cortical gray matter and signal uniformity on T1-weighted, T2-weighted, and FLAIR images. Interpretation was based on the majority of the tumor area. Similarly, on T1-weighted postcontrast images, degree of CE was evaluated and classified based on the pattern of the largest portion of the tumor. Peritumoral edema was graded and cystic structures noted according to a previous study.[31] Subarachnoid CSF signal loss, midline shift, ventricular distortion, brain herniations, and syringohydromyelia were all categorized

TABLE 1 Summary of clinical signs annotation

Clinical finding	Descriptions used in this study (total number of cases for each criterion)
Seizures	None (35); isolated (32); cluster seizures (24)
Mentation	Normal (28); lethargy/disorientation (14); depression (48)
Behavior	Normal (44); behavioral abnormalities (46)
Posture	Normal (69); head tilt (11); head turn (2); low-head carriage (6); kyphosis (1)
Gait	Normal (37); ataxia, paresis, or both (53)
Proprioception	Normal (23); deficits (67)
Vision	Normal (41); unilateral deficits (34); bilateral deficits (15)
Facial/nasal sensation	Normal (81); deficits (9)
Brainstem signs	Yes (facial asymmetry (3); abnormal eye movements/position (10); anisocoria (3); pupillary light reflex deficits (3)); no (75)
Hyperesthesia	Yes (14); no (76)

TABLE 2 Standardized MRI interpretation criteria for intracranial gliomas included in this study (n = 74)

MRI criteria	Descriptions used in this study (total number of cases for each criterion)
Origin	Intra-axial (72); extra-axial (2)
Margins	Poorly defined (25); smooth (44); irregular (5)
Shape	Spherical or ovoid/elongate (47); amorphous (24); lobulated (3)
Signal	
T2-intensity	Hypointense (3); isointense (0); hyperintense (71)
T2-uniformity	Homogeneous (22); heterogeneous (52)
T1-intensity	Hypointense (60); isointense (14); hyperintense (0)
T1-uniformity	Homogeneous (15); heterogeneous (59)
FLAIR intensity	Hypointense (11); isointense (0); hyperintense (63)
FLAIR uniformity	Homogeneous (16); heterogeneous (58)
GRE signal voids[a]	None (25); single (6); multiple (6); diffuse (majority of tumor) (4)
Degree of CE	None (19); mild (20); moderate (19); severe (16)
CE pattern	None (19); focal (1); nonuniform (28); uniform (entire tumor) (8); partial ring (7); complete ring (11)
Cystic structures	None (44); cyst (16); ITFs (14)
Peritumoral edema	None (7); peritumoral (≤10 mm beyond tumor margins) (47); extensive (>10 mm beyond tumor margins) (20)
Mass effect	None (3); mild (16); moderate (29); severe (26)
Subarachnoid CSF signal loss	Yes (63); no (11)
Midline shift	Yes (54); no (20)
Ventricular distortion	Yes (68); no (6)
Brain herniations[b]	None (31); subfalcine (2); transtentorial (24); foramen magnum (19)
Syringohydromyelia	Yes (24); no (50)
Spread	
Adjacent brain structures	None (22); butterfly glioma (3); gliomatosis cerebri growth pattern (5); freehand description (44)
Brain surface contact	Yes (56); no (18)
Leptomeningeal CE	Yes (25); no (49)
Ventricular contact	Yes (62); no (12)
CSF pathways[b]	None (26); subarachnoid space (25); ventricular invasion (33); drop metastases (8)
Other structures[b]	None (60); penetration of bone (9); other (freehand description) (6)

Abbreviations: CE, contrast enhancement; CSF, cerebrospinal fluid; FLAIR, fluid-attenuation inversion recovery; GRE, gradient-recalled echo; ITFs, intratumoral accumulations of fluid; MRI, magnetic resonance imaging; T1, T1-weighted; T2, T2-weighted.
[a]GRE images were only obtained in 41 gliomas.
[b]More than 1 criterion could be observed for a single case.

independently and subsequently considered for mass effect grading.[14,32]

Additionally, brain MRIs were evaluated for features of tumor spread, categorized as specified in Table 2. For spread from the anatomic location containing the largest fraction of the tumor to neighboring brain structures or distant foci, observers were instructed to provide a freehand description of the anatomic region/s tumors were extending to. Tumor growth patterns consistent with butterfly glioma or gliomatosis cerebri were recorded.[19,24,25] Leptomeningeal CE with associated FLAIR hyperintensity within the sulci was recorded as well.[25,26] When present, this was also annotated as extension into the subarachnoid space as was tumor invasion of the subarachnoid space without associated meningeal MRI changes. Spread along the CSF pathways including ventricular invasion and drop metastases was noted too.[26-29] Similarly, propagation to non-CNS structures was recorded.

Finally, based on the observations of published MRI predictors of canine glioma type and grade (summarized in Supplementary Table 2), investigators predicted the grade (high or low) and type (astrocytoma or oligodendroglioma) for each tumor.[13-15] Accuracy for predicting the lesion grade and type on MRI compared to histopathologic diagnosis was performed using the consensus opinion of both observers.

2.5 | Treatment and outcome

Treatment groups were defined as definitive if specific treatment modalities including surgical resection, radiotherapy, or chemotherapy were used in any combination, and palliative if corticosteroid, antiepileptic, or analgesic medications were the only therapeutic

interventions.[33] Survival was defined for all cases from time of MRI diagnosis, and only for cases with survival times >1 day to exclude animals euthanized at the time of diagnosis.[33]

2.6 | Statistical analyses

All analyses were carried out using SAS 9.4 (SAS Institute Inc, Cary, North Carolina) and R 4.0.2 (R Foundation for Statistical Computing, Vienna, Austria). When not specified, alpha level for determination of significance was .05 and trends were discussed for alpha .1.

Interobserver agreement for each MRI criterion was assessed using Cohen's kappa. Values of 0.81-1.00 were considered to indicate excellent agreement; 0.61-0.80, good agreement; 0.41-0.60, moderate agreement; 0.21-0.40, fair agreement; 0.01-0.20, poor agreement, and 0.00, chance agreement.

Agreement between histopathologic diagnosis (reference test) of type and grade and classification of glioma type and grade following previously published MRI criteria[13,14] was analyzed using specificity and sensitivity for detection of astrocytoma for type and high for grade.

Associations between tumor location, patient demographics, clinical signs, MRI criteria, and tumor type and grade were performed in 2 stages, first univariate analysis, and then multivariable analysis. Univariate analysis was done using contingency tables and Fisher's exact test. Variables with *P* value <.25 were used for the multivariable model. For multivariable analysis, forward stepwise logistic regression was used. A *P*-value to enter the model of <.20 and to remain of <.05 was used. Final logistic regression model fit was evaluated using the Hosmer-Lemeshow goodness-of-fit test.

Associations between all risk factors and hazard of death was performed for dogs with survival of >1 day and available MRI for revision using univariable followed by multivariable Cox proportional hazard modeling. All risk factors with a *P* value <.25 in the univariate analysis were used in the multivariable analysis. A forward stepwise manual approach was used to build the multivariable model. Risk factors were kept in the final model after assessing for confounding with a *P* value of .05. The proportional hazards assumption was tested by visual inspection of log-minus-log survival plots and statistical assessment of residuals.

3 | RESULTS

3.1 | Morphologic diagnosis

Ninety-one dogs with histopathological diagnosis of glioma were identified. Ten cases were identified by surgical biopsy and 81 cases were diagnosed at necropsy. Of these, 68.1% were classified as oligodendroglioma (52 high-grade and 10 low-grade), 18.7% as astrocytoma (16 high-grade and 1 low-grade), and 13.2% as undefined glioma (12, all high-grade).

Immunohistochemistry results for GFAP were available for 60 cases with a mean immunoreactivity score of 0.32/4 (range, 0-2/4) on 35 oligodendrogliomas, 1.71/4 (range, 0-4/4) on 14 astrocytomas, and 1.55/4 (range, 0-4/4) on 11 high-grade undefined gliomas (HUs). Olig2 immunoreactivity results were available for 57 cases with mean scores of 2.67/4 (range, 1-4/4) on 36 oligodendrogliomas, 1.85/4 (range, 0-4/4) on 13 astrocytomas, and 2/4 (range, 1-3/4) on 8 HUs.

Information on histopathologically confirmed infiltrative spread was available for 75 cases. Invasion of neighboring brain structures was observed in 51/75 cases including 35 oligodendrogliomas (32 high-grade and 3 low-grade), 10 high-grade astrocytomas (HAs), and 6 HUs. Secondary structures of Scherer were noted in 28/75 cases: 19 oligodendrogliomas (18 high-grade and 1 low-grade), 6 HAs, and 3 HUs. These consisted of perivascular satellitosis and subpial tumor cell condensation (9 cases, respectively), and perineuronal satellitosis, subependymal tumor cell condensation, and white matter tract invasion (7 cases, respectively) in any combination. Three high-grade oligodendrogliomas (HOs) presented as butterfly gliomas (Figure 1A-C) whereas gliomatosis cerebri growth pattern was seen in 3 HAs and 1 HU.

Ventricular invasion was confirmed in 24/75 cases (18 HOs, 4 HAs, 1 HU, and the only low-grade astrocytoma [LA]). Subarachnoid spread with or without proliferation within the leptomeninges was noted in 22/75 gliomas (16 HOs, 4 HAs, and 2 HUs). Drop metastases were found in 9 HOs and 1 HA. Additionally, 1 HA presented 2 independent foci (Figure 1D-G).

Information on spread to non-CNS structures and extraneural metastases was available in 50 cases. Penetration of the cribriform plate and infiltration of the ethmoturbinates and nasal mucosa was confirmed in 3 HOs whereas osteolytic calvarial invasion was noted on a previously reported HA.[21] Pituitary gland infiltration (Figure 1H-J) was found in 1 of each of HA, HO, and low-grade oligodendroglioma (LO). No metastases were found elsewhere in the body.

3.2 | Location of gliomas within the CNS

There were 69/91 (76%) hemispheric gliomas, 14/91 (15%) diencephalic, 5/91 (6%) infratentorial, and 3/91 (3%) in the spinal cord. Geographic distribution within the brain of type and grade of glioma is summarized in Figure 2A. Within the cerebral hemispheres (Figure 2B), 29/69 tumors (42%) had a fronto-olfactory location, 25/69 (36%) were in the temporal lobe, 11/69 (16%) in the parietal lobe, and 4/69 (6%) were primarily intraventricular. All of the latter were located within the lateral ventricles and consisted of HOs. In addition to the 14 primarily diencephalic gliomas, another 16 gliomas involved the diencephalon to some extent (diencephalic involvement by tumor type and grade is presented in Table 3). Infratentorial gliomas included 4 HAs (brainstem, 3; cerebellum, 1) and 1 HO (brainstem). Spinal cord gliomas consisted of 2 HOs located at the level of C1 and T11 vertebrae, respectively, and 1 LO extending from C7 to T5 vertebral bodies.

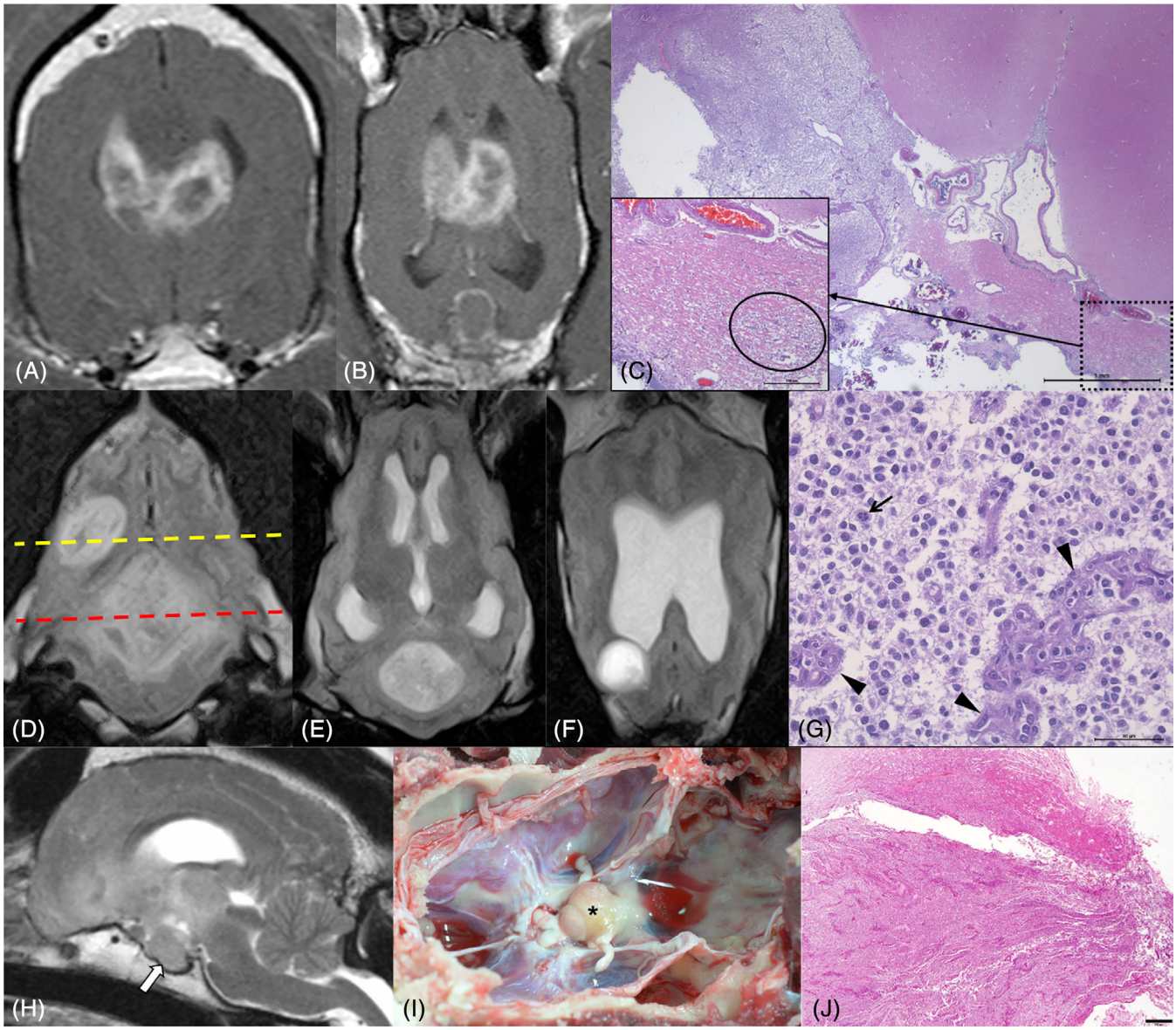

FIGURE 1 Transverse (A) and dorsal (B) T1-weighted postcontrast magnetic resonance (MR) images of a ring-enhancing high-grade oligodendroglioma (HO) showing the typical features of butterfly glioma with extensive involvement of the corpus callosum leading to bihemispheric spread. Photomicrograph of the same HO as in (A) and (B) occupying the lumen of the lateral ventricle and infiltrating the cingulate gyrus (top of the figure) and the corpus callosum (bottom of the figure) (C). The inset shows neoplastic cells invading the corpus callosum towards the contralateral ventricle (the oval represents an area of higher neoplastic cell density). HE stain. Scale bar = 1 mm (inset 200 μm). Transverse fluid-attenuation inversion recovery MR image at the level of the tentorium cerebelli demonstrating 2 heterogeneously hyperintense independent foci of a high-grade astrocytoma (D). Dorsal T2-weighted images obtained at the level of the red (E) and the yellow (F) dotted lines show the largest tumor in the cerebellum and a second focus in the right occipital lobe, respectively. Both foci were characterized by large sized anisokaryotic cell populations with scant cytoplasm growing in a solid pattern (G). A mitotic figure is present (arrow) as well as glomeruloid-like vessels (arrowheads). HE stain. Scale bar = 50 μm. Midsagittal T2-weighted images of a poorly defined, heterogeneously hyperintense HO extending from the fronto-olfactory area to the diencephalon (H). Note the enlarged and hyperintense pituitary gland (arrow). Severe nonuniform enhancement of the pituitary gland was noted on T1-weighted postcontrast images whereas this was mild for the intra-axial tumor. Dorsal view of the unfixed base of the neurocranium in the same dog as (H) demonstrating an expanded pituitary gland (asterisk) (I). Photomicrograph of the pituitary gland of the dog in (H) and (I) revealing severe infiltration of the hypophyseal lobules by the neoplastic cell population (J). HE stain. Scale bar = 500 μm

3.3 | Demographics, clinicopathologic features, and staging

Median age of dogs at diagnosis of glioma was 7.9 years (range, 1.5-13.0 years). There were 40/91 (44%) intact males, 11/91 (12%) castrated males, 21/91 (23%) intact females, and 19/91 (21%) spayed females. The ratio for all males/females was 1.28, and 1.9 for intact males/females. Seventy-eight percent of the cases (71/91) belonged to brachycephalic dog breeds including 40/91 (44%) Boxers, 26/91 (29%) Bulldogs (French, 23; English, 1; and not otherwise specified, 2),

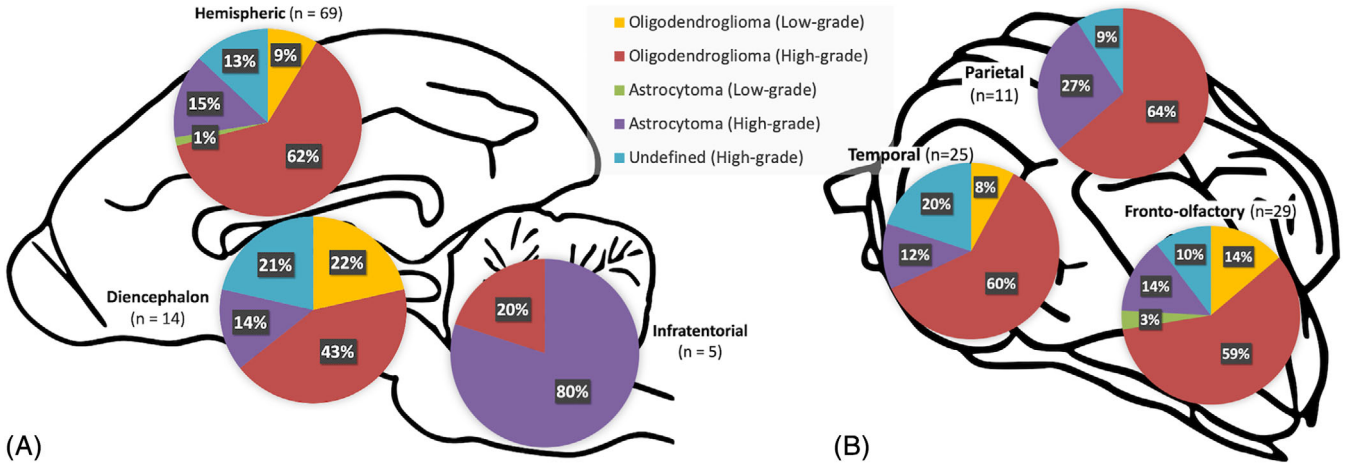

FIGURE 2 Anatomic distribution of intracranial gliomas in 88 dogs classified according to the Comparative Brain Tumor Consortium diagnostic scheme (A). Specific location of 65 hemispheric gliomas (B). Note there were an additional 4 high-grade oligodendrogliomas primarily located within the lateral ventricles

3/91 (3%) Dogues de Bordeaux, and 2/91 (2%) Staffordshire Bull Terriers. The breeds of the remaining 22% of dogs are captured on Supplementary Table 1.

Time between onset of clinical signs and presentation ranged between <1 and 180 days (median 14 days) for all gliomas. The main presenting complaint in 62% (56/91) of the cases was seizures either isolated (32 dogs) or in clusters (24). Of these, 5/56 (9%) presented with a normal interictal neurologic examination and seizures as the only clinical sign. In addition to seizures, the most common presenting neurologic signs included proprioceptive deficits (67/90 cases, 74%), mentation changes (62/90 cases, 69%), gait abnormalities (53/90 cases, 59%), visual deficits (49/90 cases, 54%), and behavioral changes (46/90 cases, 51%). The remaining clinical signs are outlined in Table 1 and most common neurologic signs by tumor type and grade are presented in Table 3.

Cerebrospinal fluid was collected in 23 dogs. The results are summarized in Table 4. These were within reference limits in 31.6% (6/19), consistent with albuminocytologic dissociation in 36.8% (7/19) and with an elevated total nucleated cell count in 34.8% (8/23) cases. Mixed cell pleocytosis was the most common cytologic abnormality. No neoplastic cells were detected. Thoracic radiographs (40 cases) and CT (8), as well as abdominal ultrasonography (40 cases) or CT (3), failed to reveal abnormalities suggestive of metastatic disease.

3.4 | Magnetic resonance imaging

Magnetic resonance imaging was obtained for diagnosis in 87 dogs. The remaining 4 dogs were euthanized on presentation at their owners request in view of the clinical suspicion and severity of clinical signs. The MRI studies of 77 cases were available for review, including 74 brain and 3 spinal cord gliomas. Median time between MRI and postmortem examination was 1 day (range, <1-1104 days). All brain studies included FLAIR sequences whereas GRE images were attained on 41.

Magnetic resonance imaging features of spinal cord gliomas consisted of T2-weighted hyperintense, T1-weighted isointense focal, or diffuse mass lesions with none to severe CE located intramedullary except for the HO at C1 that appeared intradural extramedullary (Figures 3A-C).

The MRI features of intracranial gliomas are captured in Table 2. All intracranial gliomas in this study were intra-axial except for a HA (Figures 3D-F) and a previously reported case of leptomeningeal oligodendrogliomatosis reclassified as HO.[22] Spread to adjacent brain structures was detected in 52/74 (70%) gliomas and further characterized as butterfly glioma in 3 HOs and as gliomatosis cerebri growth pattern in 4 HAs and 1 HU. Extension outside the CNS including penetration into the bone and invasion of the pituitary gland was suspected in 9/74 and 6/74 gliomas, respectively. The MRI findings by tumor type and grade are presented in Table 5.

Supplementary Figure 1 shows the interobserver agreement for all the MRI variables studied. Kappa values were excellent or good in most cases except for predicted tumor grade and spread to bone structures that showed moderate agreement, and poor for predicted tumor type.

Evaluation of previously published criteria[13,14] for prediction of intracranial glioma type and grade demonstrated a sensitivity of 58.8% (95% confidence interval [CI], 35.4%-82.2%) and specificity of 68.8% (95% CI, 55.6%-81.8%) for the diagnosis of astrocytoma, and a sensitivity of 67.2% (95% CI, 55.2%-79.3%) and specificity 57.1% (95% CI, 20.5%-93.8%) for the diagnosis of high-grade.

3.5 | Associations among tumor location, demographics, clinical signs, MRI features, and glioma type and grade

The preliminary univariate analysis (Tables 3 and 5) showed associations between glioma type and presence of facial or nasal sensation

TABLE 3 Univariate analysis of tumor location, patient demographics, and clinical features of 91 gliomas based on type and grade. Table shows percentage of each criterion within each type or grade (total number of cases for each criterion)

	Type				Grade		
	Astrocytoma (n = 17)	Oligodendroglioma (n = 62)	Undefined (n = 12)	*P* value	High (n = 80)	Low (n = 11)	*P* value
Location							
Diencephalon	11.8 (2)	14.5 (9)	25.0 (3)	.07	13.8 (11)	27.3 (3)	.28
Hemispheric	64.7 (11)	79.0 (49)	75.0 (9)		77.5 (62)	63.6 (7)	
Infratentorial	23.5 (4)	1.6 (1)	0 (0)		6.3 (5)	0 (0)	
Spinal cord	0 (0)	4.9 (3)	0 (0)		2.5 (2)	9.1 (1)	
Diencephalic involvement	29.4 (5)	33.9 (21)	33.3 (4)	.99	33.8 (27)	27.3 (3)	.99
Demographics							
Age (>96 months)	53.0 (9)	46.8 (29)	58.3 (7)	.73	50.0 (37)	45.5 (4)	.78
Sex							
F	11.8 (2)	25.8 (16)	25.0 (3)	.86	26.3 (21)	0 (0)	.06
FN	29.4 (5)	19.4 (12)	16.7 (2)		20.0 (16)	27.3 (3)	
M	41.2 (7)	43.6 (27)	50.0 (6)		40.0 (32)	72.7 (8)	
MN	17.7 (3)	11.3 (7)	8.33 (1)		13.8 (11)	0 (0)	
Boxer breed	41.2 (7)	46.8 (29)	33.3 (4)	.66	43.8 (35)	45.5 (5)	.99
Bulldog breed	35.3 (6)	25.8 (16)	33.3 (4)	.68	31.3 (25)	9.1 (1)	.17
Boxer's phylogenetic clade[34]	82.4 (14)	79.0 (49)	66.7 (8)	.64	78.7 (63)	72.7 (8)	.7
Clinical features							
Duration of signs (>3 days)	86.7 (15)	81.4 (50)	81.8 (10)	.99	79.7 (64)	100.0 (11)	.2
Seizures							
None	41.2 (7)	37.1 (23)	41.7 (5)	.87	38.8 (31)	36.4 (4)	.99
Isolated	29.4 (5)	38.7 (24)	25.0 (3)		35.0 (28)	36.4 (4)	
Cluster seizures	29.4 (5)	24.2 (15)	33.3 (4)		26.3 (21)	27.3 (3)	
Mentation							
Normal	11.8 (2)	36.1 (22)	33.3 (4)	.21	27.9 (22)	54.6 (6)	.08
Lethargy/disorientation	11.8 (2)	14.8 (9)	25.0 (3)		15.2 (12)	18.2 (2)	
Depression	76.5 (13)	49.2 (30)	41.7 (5)		57.0 (45)	27.3 (3)	
Behavioral abnormalities	58.8 (10)	47.5 (29)	58.3 (7)	.62	51.9 (41)	45.5 (5)	.76
Kyphosis/low-head carriage	5.9 (1)	8.2 (5)	8.3 (1)	.99	7.6 (6)	9.1 (1)	.99
Head tilt or turn	29.4 (5)	11.5 (7)	8.3 (1)	.21	16.5 (13)	0 (0)	.36
Gait abnormalities	47.1 (8)	62.3 (39)	50.0 (6)	.42	58.2 (47)	54.6 (6)	.99
Proprioceptive deficits	70.6 (12)	70.5 (44)	91.7 (11)	.36	74.7 (60)	63.6 (7)	.48
Vision							
Normal	64.7 (11)	44.3 (27)	25.0 (3)	.29	43.0 (34)	63.6 (7)	.27
Unilateral deficits	29.4 (5)	37.7 (23)	50.0 (6)		38.0 (30)	36.4 (4)	
Bilateral deficits	5.9 (1)	18.0 (11)	25.0 (3)		19.0 (15)	0 (0)	
Facial/nasal sensation deficits	11.8 (2)	4.9 (3)	33.3 (4)	.01	10.1 (8)	9.1 (1)	.99
Facial asymmetry	0 (0)	4.9 (3)	0 (0)	.99	3.8 (3)	0 (0)	.99
Abnormal eye movements/position	11.8 (2)	13.1 (8)	0 (0)	.52	11.4 (9)	9.1 (1)	.99
Anisocoria/PLR deficits	11.8 (2)	6.6 (4)	0 (0)	.55	7.6 (6)	0 (0)	.99
Hyperesthesia	17.7 (3)	14.8 (9)	16.7 (2)	.91	17.7 (14)	0 (0)	.2

Abbreviations: F, female; FN, female neutered; M, male; MN, male neutered; PLR, pupillary light reflex.

TABLE 4 CSF analysis results by tumor type and grade in dogs with glioma[5]

Tumor type and grade[a]	Elevated TP concentration[b]	Elevated TNCC[c]	ACD[d]	Normal CSF[a]	Mean TP concentration and range (mg/dL)	Mean TNCC and range (cells/μL)	Differential cytology
LO (3)	1 (2)	1 (3)	1 (2)	1 (2)	23.3 (20-26.5)	28 (1-81)	Eosinophilic pleocytosis, 1[e]
HO (13)	8 (11)	3 (13)	6 (11)	3 (11)	143.0 (10.1-780)	38 (0-460)	Increased percentage of neutrophils (62%), 1[f]; Mixed cell pleocytosis, 3[g]
HA (4)	3 (4)	3 (4)	0 (4)	1 (4)	206.1 (22.5-736)	15 (0-27)	Mixed cell pleocytosis, 3
HU (3)	1 (2)	1 (3)	0 (2)	1 (2)	75.1 (20-130.2)	10 (0-27)	Neutrophilic pleocytosis, 1[h]

Abbreviations: ACD, albuminocytologic dissociation; CSF, cerebrospinal fluid; HA, high-grade astrocytoma; HO, high-grade oligodendroglioma; HU, high-grade undefined glioma; LO, low-grade oligodendroglioma; TNCC, total nucleated cell count; TP, total protein.
[a]Number of cases in which CSF information was available.
[b]Number of cases with >25 mg/dL TP concentration (number of cases with available information).
[c]Number of cases with >5 cells/μL (number of cases with available information).
[d]Number of cases with >25 mg/dL TP concentration and <5 cells/μL (number of cases with available information).
[e]Defined as CSF with >50% eosinophils.
[f]Defined as CSF >2% nondegenerated neutrophils.[35]
[g]Defined as CSF with a mixture of mostly lymphocytes and large mononuclear cells and >20% contribution of neutrophils and, occasionally, eosinophils.[35]
[h]Defined as CSF with >75% neutrophils.

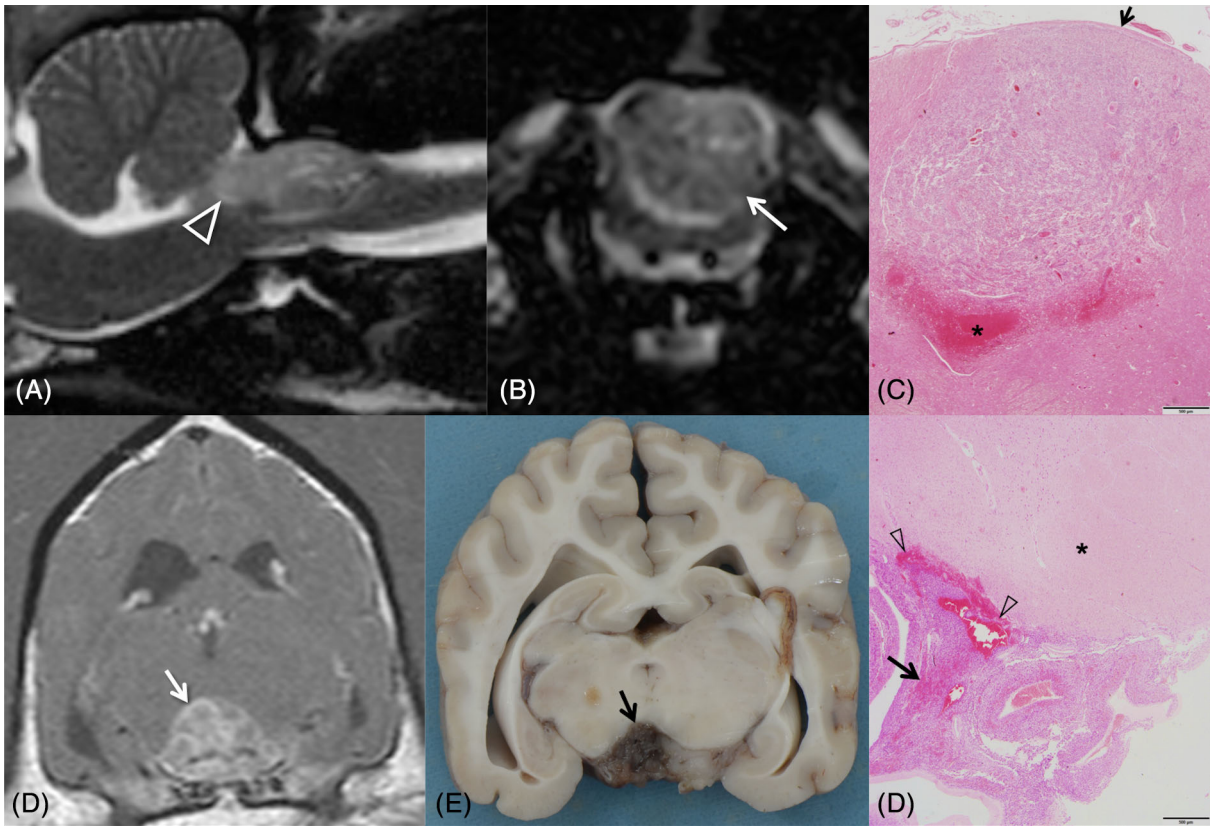

FIGURE 3 Midsagittal (A) and transverse (B) T2-weighted magnetic resonance (MR) images of a heterogeneously hyperintense high-grade oligodendroglioma at the level of C1 vertebra (arrow) identified as intradural-extramedullary by both observers. Note the mass extension into the foramen magnum (arrowhead). Photomicrograph of the same tumor as (A) and (B) demonstrating a highly cellular proliferation in direct contact with the thickened pia mater (arrow) in the dorsal aspect of the spinal cord (C). Note the severe hemorrhages ventrally where the mass is compressing the spinal cord parenchyma (asterisk). HE stain. Scale bar = 500 μm. Transverse T1-weighted postcontrast MR image of an extra-axial nonuniformly contrast-enhancing high-grade astrocytoma ventral to the mesencephalon (arrow) (D). Formalin-fixed transverse section of the brain at the level of (D) demonstrating the extra-axial appearance of the tumor (arrow) (E). Photomicrograph of the paraffin-embedded tumor in (D) and (E) showing a highly cellular proliferation spreading through the subarachnoid space ventral to the mesencephalon (asterisk) with multiple foci of hemorrhage (arrowheads) and necrosis (arrow) (F). HE stain. Scale bar = 500 μm

TABLE 5 Univariate analysis of MRI criteria of 74 intracranial gliomas based on type and grade. Table shows percentage of each criterion within each type or grade (total number of cases for each criterion)

	Type				Grade		
	Astrocytoma (n = 17)	Oligodendroglioma (n = 49)	Undefined (n = 8)	*P* value	High (n = 67)	Low (n = 7)	*P* value
Margins							
Smooth	47.1 (8)	69.4 (34)	25.0 (2)	.02	56.7 (38)	85.7 (6)	.53
Irregular	11.8 (2)	2.0 (1)	25.0 (2)		7.5 (5)	0 (0)	
Poorly defined	41.2 (7)	28.6 (14)	50.0 (4)		35.8 (24)	14.3 (1)	
Shape							
Amorphous	29.4 (5)	28.6 (14)	62.5 (5)	.09	34.3 (23)	14.3 (1)	.24
Lobulated	5.9 (1)	2.0 (1)	12.5 (1)		3.0 (2)	14.3 (1)	
Spherical or ovoid/elongate	64.7 (11)	69.4 (34)	25.0 (2)		62.7 (42)	71.4 (5)	
Signal							
T2-hypointensity[a]	11.8 (2)	2.0 (1)	0 (0)	.26	4.5 (3)	0 (0)	.99
T2-homogeneity	29.4 (5)	32.7 (16)	12.5 (1)	.63	28.4 (19)	42.9 (3)	.42
T1-hypointensity[b]	47.1 (8)	95.9 (47)	62.5 (5)	<.001	80.6 (54)	85.7 (6)	.99
T1-homogeneity	29.4 (5)	14.3 (7)	37.5 (3)	.15	19.4 (13)	28.6 (2)	.62
FLAIR hypointensity[c]	11.8 (2)	16.3 (8)	12.5 (1)	.99	14.9 (10)	14.3 (1)	.99
FLAIR homogeneity	29.4 (5)	16.3 (8)	37.5 (3)	.23	22.4 (15)	14.3 (1)	.99
GRE signal voids[d]	50.0 (5)	37.0 (10)	25.0 (1)	.7	41.0 (16)	0 (0)	.51
Contrast enhancement							
Moderate to severe[e]	58.8 (10)	44.9 (22)	37.5 (3)	.56	49.3 (33)	28.6 (2)	.43
CE pattern							
No CE	17.7 (3)	27.5 (14)	25.0 (2)	.42	22.1 (15)	50.0 (4)	.37
Partial or complete ring	23.5 (4)	27.5 (14)	0 (0)		25.0 (17)	12.5 (1)	
Other patterns	58.8 (10)	42.9 (21)	75.0 (6)		50.7 (34)	37.5 (3)	
Tumor characteristics							
Cystic structures	41.2 (7)	42.9 (21)	25.0 (2)	.72	40.3 (27)	42.9 (3)	.99
Peritumoral edema							
None	5.9 (1)	12.2 (6)	0 (0)	.28	9.0 (6)	14.3 (1)	.84
Peritumoral	47.1 (8)	67.4 (33)	75.0 (6)		64.2 (43)	57.1 (4)	
Extensive	47.1 (8)	20.4 (10)	25.0 (2)		26.9 (18)	28.6 (2)	
Mass effect							
None	11.8 (2)	2.0 (1)	0 (0)	.11	4.5 (3)	0 (0)	.11
Mild	17.7 (3)	26.5 (13)	0 (0)		20.9 (14)	28.6 (2)	
Moderate	23.5 (4)	44.9 (22)	37.5 (3)		35.8 (24)	71.4 (5)	
Severe	47.1 (8)	26.5 (13)	62.5 (5)		38.8 (26)	0 (0)	
Subarachnoid CSF signal loss	88.2 (15)	81.6 (40)	100.0 (8)	.62	85.1 (57)	85.7 (6)	.99
Midline shift	64.7 (11)	73.5 (36)	87.5 (7)	.52	71.6 (48)	85.7 (6)	.66
Ventricular distortion	88.2 (15)	91.8 (45)	100.0 (8)	.82	91.0 (61)	100.0 (7)	.99
Brain herniations							
None	35.3 (6)	44.9 (22)	37.5 (3)	.09	41.8 (28)	42.8 (3)	.21
Transtentorial or subfalcine	41.2 (7)	34.7 (17)	0 (0)		29.9 (20)	57.1 (4)	
Foramen magnum	23.5 (4)	20.4 (10)	62.5 (5)		28.4 (19)	0 (0)	
SHM	35.3 (6)	30.6 (15)	37.5 (3)	.8	35.8 (24)	0 (0)	.09
Spread							
Adjacent brain structures	58.8 (10)	69.4 (34)	100.0 (8)	.09	74.6 (50)	28.6 (2)	.02

TABLE 5 (Continued)

	Type				Grade		
	Astrocytoma (n = 17)	Oligodendroglioma (n = 49)	Undefined (n = 8)	*P* value	High (n = 67)	Low (n = 7)	*P* value
Brain surface contact	76.5 (13)	77.6 (38)	62.5 (5)	.65	74.6 (50)	85.7 (6)	.99
Leptomeningeal CE	47.1 (8)	28.6 (14)	37.5 (3)	.34	35.8 (24)	14.3 (1)	.26
Ventricular contact	64.7 (11)	87.8 (43)	100.0 (8)	.05	83.6 (56)	85.7 (6)	.99
CSF pathways							
Subarachnoid space	47.1 (8)	28.6 (14)	37.5 (3)	.34	35.8 (24)	14.3 (1)	.41
Ventricular invasion	23.5 (4)	49.0 (24)	62.5 (5)	.09	46.3 (31)	28.6 (2)	.45
Drop metastases	0 (0)	16.3 (8)	0 (0)	.16	11.9 (8)	0 (0)	.99
Other structures							
Pituitary gland	5.9 (1)	8.2 (4)	12.5 (1)	.82	7.5 (5)	14.3 (1)	.46
Penetration of bone	17.7 (3)	12.2 (6)	0 (0)	.56	13.4 (9)	0 (0)	.59

Abbreviations: CE, contrast enhancement; CSF, cerebrospinal fluid; FLAIR, fluid-attenuation inversion recovery; GRE, gradient-recalled echo; MRI, magnetic resonance imaging; SHM, syringohydromyelia; T1, T1-weighted; T2, T2-weighted.

[a]As opposed to T2-weighted hyperintensity seen in 88.2% (15) astrocytomas, 98% (48) oligodendrogliomas, and all undefined gliomas; 95.5% (64) high-grade gliomas and all low-grade gliomas.

[b]As opposed to T1-weighted isointensity seen in 52.9% (9) astrocytomas, 4.1% (2) oligodendrogliomas, and 37.5% (3) undefined gliomas; 19.4% (13) high-grade gliomas and 14.3% (1) low-grade gliomas.

[c]As opposed to FLAIR hyperintensity seen in 88.2% (15) astrocytomas, 83.7% (41) oligodendrogliomas, and 87.5% (7) undefined gliomas; 85.1% (57) high-grade gliomas and 85.7% (6) low-grade gliomas.

[d]Percentages and total number of cases with signal voids out of 41 gliomas where GRE images were obtained.

[e]As opposed to none to mild CE seen in 41.2% (7) astrocytomas, 55.1% (27) oligodendrogliomas, and 62.5% (5) undefined gliomas; 50.7% (34) high-grade gliomas and 71.4% (5) low-grade gliomas.

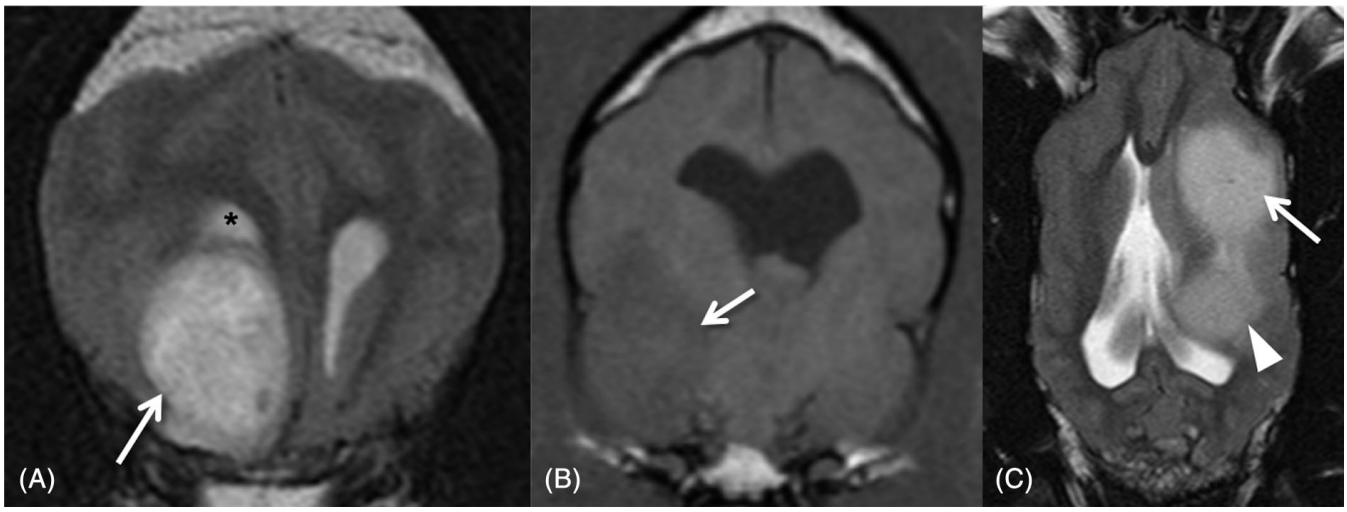

FIGURE 4 Transverse T2-weighted magnetic resonance (MR) image of a high-grade oligodendroglioma (HO) in the right frontal lobe (arrow) with smooth margins and in close contact with the lateral ventricle (asterisk) (A). Transverse T1-weighted image of a hypointense to gray matter HO in the right temporal lobe (arrow) (B). Dorsal T2-weighted MR image showing a high-grade undefined glioma extending from the frontal (arrow) to the temporal lobe (arrowhead) (C). Involvement of the parietal lobe and hippocampus were also noted and gliomatosis cerebri growth pattern was subsequently confirmed on histopathology

deficits ($P = .01$), tumor margins ($P = .02$) on MRI, T1-weighted signal intensity ($P < .001$), and ventricular contact ($P = .04$).

Multivariable logistic regression analysis indicated that oligodendrogliomas were more often associated with smooth margins (Figure 4A) than astrocytomas (odds ratio [OR], 42.5; 95% CI, 2.42-744.97; $P = .04$) or undefined gliomas (OR, 84; 95% CI, 3.43-999.99; $P = .02$). Oligodendrogliomas were also associated with T1-weighted hypointensity (Figure 4B) in comparison with astrocytomas (OR, 45.5;

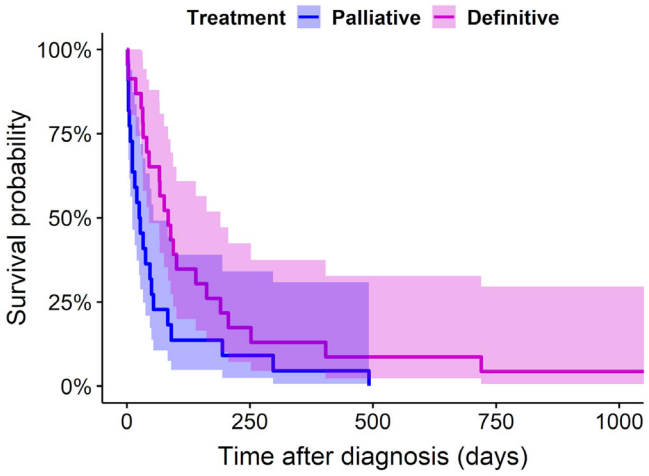

FIGURE 5 Kaplan-Meier survival curve for definitively and palliatively treated dogs with intracranial glioma that survived >1 day (n = 45). Dogs receiving definitive treatment survived significantly longer ($P = .03$) than did dogs with palliative treatment. Survival time represents the time from diagnosis to death or euthanasia. Shadow areas represent 95% confidence intervals

95% CI, 5.78-333.33; $P < .001$) or undefined gliomas (OR, 32.3; 95% CI, 2.51-500.00; $P = .008$). Finally, oligodendrogliomas were more often in contact with the ventricles (Figure 4A) than astrocytomas (OR, 7.47; 95% CI, 1.03-53.95; $P = .049$).

For tumor grade, the univariate analysis (Tables 3 and 5) showed associations with spread to adjacent brain structures ($P = .02$).

The multivariable logistic regression analysis indicated that spread to neighboring brain structures (Figure 4C) was more often associated with high-grade gliomas (OR, 6.02; 95% CI, 1.06-34.48; $P = .04$).

3.6 | Treatment and outcome

Survival time was available for all 87 dogs undergoing MRI for diagnosis. Forty-two dogs survived <1 day (euthanized at diagnosis) and were excluded from further analysis to remove cases without intent to treat. Of the 45 dogs that survived >1 day, 22 received palliative treatment (10 HOs, 6 HAs, 3 HUs, and 3 LOs), and 23 received definitive treatment (11 HOs, 5 HUs, 3 HAs, 3 LOs, and 1 LA). Treatment modalities and survival data are outlined in Supplementary Table 1.

TABLE 6 Multivariable Cox proportional hazard ratios for the survival analysis of 36 dogs surviving >1 day after imaging diagnosis and available MRI study for evaluation

Clinical or MRI variable	*P* value	Hazard ratio	95% confidence interval
Seizures	<.001	0.044	0.011-0.173
Margins[a]			
Irregular	.001	31.69	4.23-237.28
Poorly defined	.003	7.57	2.04-22.18
Drop metastases	<.001	53.15	6.25-452.22
T2-heterogeneity	.001	6.93	2.21-21.73

Abbreviations: MRI, magnetic resonance imaging; T2-heterogeneity, T2-weighted heterogeneity.
[a]Reference category: smooth margins.

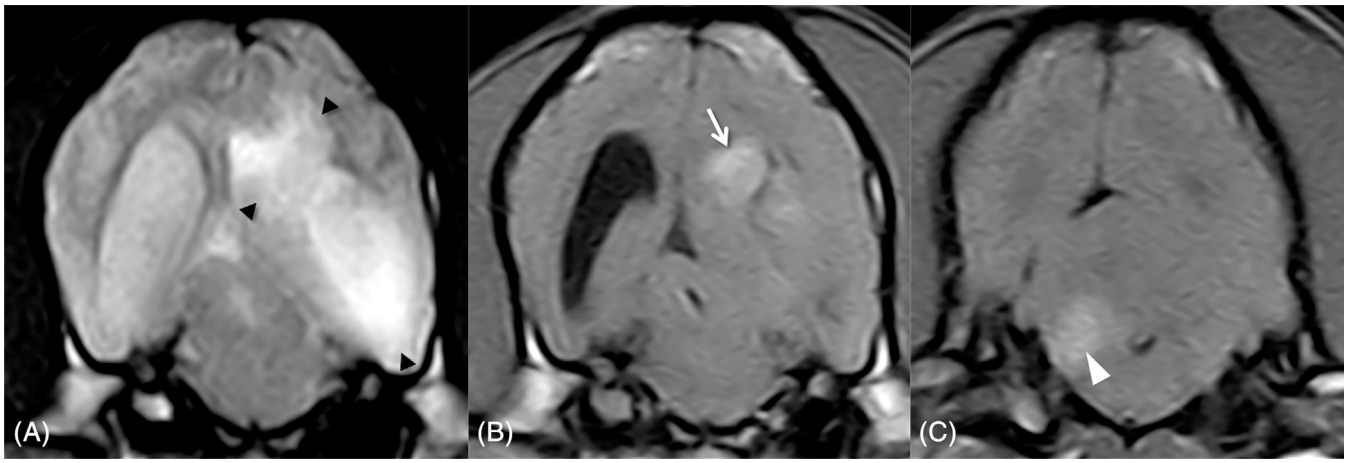

FIGURE 6 Transverse T2-weighted magnetic resonance (MR) image of a left temporal lobe high-grade oligodendroglioma (arrowheads) with poorly defined margins and heterogeneously hyperintense signal extending to the parietal lobe and invading the adjacent lateral ventricle (A). Transverse T1-weighted postcontrast image at the same level demonstrating moderate non-uniform contrast enhancement of the parietal portion of the tumor (arrow) (B). Transverse T1-weighted postcontrast image of the same dog demonstrating a contrast-enhancing drop metastasis in the right cerebellum (arrowhead), just dorsal to the lateral aperture of the fourth ventricle (C)

Among the >1-day survivors, definitive treatments were associated with significantly ($P = .03$) longer survival (median survival time [MST], 84 days; 95% CI, 45-190) than palliative treatment (MST, 26 days; 95% CI, 11-54) (Figure 5).

Univariate survival analysis is presented in Supplementary Table 3. The multivariable Cox proportional hazards model included seizures (hazards ratio [HR] 95% CI, 0.01-0.17) as a lower risk factor, and irregular (HR 95% CI, 4.2-237.3) or poorly defined (HR 95% CI, 2.0-22.2) margins, T2-weighted heterogeneous signal (HR 95% CI, 2.21-21.7), and drop metastases (HR 95% CI, 6.3-452.2) as risk factors for shorter survival (Table 6; Figure 6). No confounding risk factors or interactions were found and no evidence of violation of the proportional hazard assumption was found.

4 | DISCUSSION

Our study provides predictive information for the clinical diagnosis of glioma type and grade as well as their prognostic outcome for affected dogs. New MRI characteristics for differentiation of glioma type and grade are identified, and clinical and imaging findings are associated with survival. Additionally, we describe previously unreported features of these CNS tumors.

Glioma type and grade relative frequency in this study is consistent with data from prior literature, indicating that oligodendroglial and high-grade tumors are the most prevalent in dogs.[3,8,36] We found no associations between glioma location and tumor type or grade; however, consistent with recent studies,[8,13] our data suggest that gliomas in dogs, like their human counterparts,[30] arise mainly in the fronto-olfactory, temporal, and parietal regions of the cerebral hemispheres. The reported increased likelihood of histologic involvement of the diencephalon in astrocytomas in dogs was not observed in our cohort.[5,13] All gliomas in dogs reported to be primarily intraventricular to date have been HOs.[8,26,37]

Almost 80% of the gliomas included herein occurred in brachycephalic dog breeds belonging to the same phylogenetic clade,[34] supporting glioma pronounced predilection for these breeds.[3,5,8-10,13] However, contrasting other reports,[8] the Boxers and Bulldogs in our study did not show a higher prevalence of oligodendroglioma, although this might have been related to smaller case numbers in our sample. No associations were found between sex and tumor type or grade, but the recently reported male sex predilection[8] was confirmed by our data and resembles the situation in humans.[30]

The most common signs of neurologic dysfunction in this series included proprioceptive deficits, mentation changes, and seizures. Over 60% of the cases were diagnosed after an inaugural seizure, resembling previous studies in dogs[4,5,38] and mirroring the situation in humans.[17,39] While no presenting clinical sign was associated with glioma type or grade, seizures at onset was identified as a favorable prognostic factor for duration of survival in both low- and high-grade gliomas. Like in human gliomas, new-onset seizures might represent an early warning sign for the presence of a brain tumor as other more subtle signs of neurologic disease in dogs might go unnoticed by their owners.[39] Definitive treatment modalities contribute to seizure control in human patients and this could have influenced the improved survival of these cases in our study; however, there were no associations between seizures at onset and treatment modality.

Although definitive diagnosis of glioma requires histopathologic analysis of tumor tissue, biopsy or resection of tumors is not always possible. Therefore, the ability to predict intracranial glioma type and grade based on MRI characteristics has recently been investigated in dogs.[13-15] However, currently published MRI findings for predicting grade and tumor type have proven inaccurate.[15] We further analyzed those MRI predictors in our larger sample and confirmed their low sensitivity and specificity. Additionally, the low agreement for predicted tumor type and grade using those features indicated high interobserver variability. These might have been related to the overlap of evaluated MRI features between tumor types and grades in our population and the high variability of described predictors within each tumor.

We assessed 74 brain MRI studies for additional indicators of glioma type and grade and found that oligodendrogliomas were associated with smooth margins and T1-weighted hypointensity compared to astrocytomas and undefined gliomas as well as more commonly in contact with the ventricles than astrocytomas. Tumor spread to neighboring brain structures was the only finding associated with high-grade diagnosis. These are in contrast with reported associations among peritumoral edema and astrocytomas, brain surface contact and oligodendrogliomas, and CE and cystic structures with tumor grade.[13,14] Conversely to previous reports,[13,14] ventricular contact alone, independent of distortion, was more common in oligodendrogliomas than astrocytomas. The only similarity between this and prior studies was the significantly low likelihood of T1-weighted hypointensity in astrocytomas,[14] which was shared by undefined gliomas in this series. Although we used comparable methodology to a previous report,[14] differing results might stem from inclusion of undefined gliomas in our series and the potentially magnified significance of individual outliers not representative of the general population in that study,[14] where statistics were performed using 155 MRI observations from 5 investigators in 31 gliomas, instead of the consensus opinion used herein.

Interobserver agreement for individual MRI features associated with glioma type and grade in our study was good to excellent; however, despite reported 89% sensitivity for MRI diagnosis of neoplastic brain disease and 93.7% specificity and 84.4% sensitivity for diagnosis of glioma in dogs, other differential diagnoses with overlapping imaging characteristics still need to be considered.[12,40]

Differently from our observations, CE on MRI and in particular, ring-enhancement, is usually associated with higher grade human gliomas.[41-43] However, human LAs and approximately 50% of LOs can show CE[44-47] and its absence does not exclude high-grade glioma.[44,48,49] On the other hand, human oligodendrogliomas are usually well demarcated and largely T1-hypointense,[50,51] and glioblastomas might extend widely to adjacent brain structures,[52] resembling our observations on canine oligodendrogliomas and high-grade gliomas, respectively.

Novel features of gliomas in dogs encountered in this study included histopathologically confirmed butterfly growth pattern in 3 HOs and pituitary gland infiltration in different glioma types. Reported human and canine butterfly gliomas to date are HAs; however, our findings indicate that, as in gliomatosis cerebri, this represents a pattern of spread rather than a distinct nosologic entity.[19,24,53] Extension of glioma to the pituitary gland had not been described in dogs and has only been confirmed once in humans.[54] Other infrequent features reported here include penetration into the bone and multifocal distribution. Multifocality as a result of CSF drop metastases occurs in oligodendrogliomas in dogs[26-28]; however, truly multiple, independent gliomas have only been described in 1 dog and are a rare presentation in humans.[55,56] Additionally, we confirmed CSF seeding in a HA in 1 dog, a dissemination pathway exhibited by less than 2% of human glioblastomas.[53] Finally, extra-axial appearance of astrocytoma had only been reported in a dog,[15] and is an infrequent observation in humans.[57,58]

Data regarding treatment and survival in dogs with histopathologically confirmed glioma is scarce and yet to be added to the new classification. The survival analysis presented here is the most complete to date; however, it has limitations inherent to the low case numbers and results should be interpreted accordingly. The multivariable analysis of available clinical and MRI findings identified prognostic factors affecting survival in intracranial gliomas in dogs for the first time. In addition to the favorable association between new-onset seizures and survival, a series of MRI features were identified as negative prognostic indicators. Poorly defined and irregular tumor margins associated death hazard was over 7 and 31 times as high as that associated with smooth margins, respectively. Tumor T2-weighted heterogeneous signal and observation of drop metastases were also associated with shorter survival. These prognostic factors differ from those reported for human gliomas; nevertheless, prognosis in humans is currently guided by isocitrate dehydrogenase mutation and 1p/19q status,[19] for which parallelisms have not been found in canine gliomas.[59-63] Case series with palliative treatment outcome information relating to glioma type or grade are lacking. Canine studies evaluating experimental therapies in >3 intracranial gliomas with detailed information on their type and grade have reported MSTs of 119 days (n = 7),[64] 224 days (n = 17),[65] 248 days (n = 8),[66] and 257 days (n = 8).[67] However, no comparisons were made between differing types or grades. Similarly, a recent study reported a MST of 66 days after surgical resection alone in 14 gliomas,[68] 8 of which were reclassified and included in this study. Thus, we decided to further evaluate therapeutic outcome in our larger sample of dogs surviving diagnosis. Despite marked variability in treatment modalities (surgery, radiotherapy, chemotherapy), MST for definitively treated cases (n = 23) was longer (84 days) than for palliative treatment cases (n = 22; 26 days), suggesting that definitive therapies provide a significant survival benefit to dogs with intracranial gliomas, although this benefit appears to be limited.

This series has some limitations intrinsic to its retrospective nature and reflects the challenges inherent to the study of gliomas in dogs, including variable MRI and treatment protocols, owner decisions to euthanize rather than natural death, and erroneous or incomplete record-keeping. Thus, the authors invite researchers to contribute to the creation of a mutually accessible international multicenter database to better enable evidence-based research in this field.

Additional limitations of the current study include the fact that necropsy samples might not be representative of the original tumor phenotype, which could change with tumor progression or be influenced by treatments administered. Also, in cases where surgical biopsies were obtained, these might have failed to reflect the overall histologic features of the glioma sampled hampering accurate classification. Finally, tumor typing and grading was established by a single pathologist which could represent a potential source of bias in view of the moderate agreement for glioma type and grade observed between the multiple pathologists contributing to the CBTC classification.[8]

In conclusion, smooth margins, T1-weighted hypointensity and ventricular contact on MRI diagnosed intracranial gliomas, could allow differentiation between oligodendrogliomas and other glial tumor types in dogs. High-grade glioma should be suspected if spread over more than 1 brain region is observed. Definitive therapies appear to improve survival time. New onset seizures are associated with a more favorable prognosis, whereas MRI observed irregular or poorly defined tumor margins, T2-weighted heterogeneity and drop metastases are negative prognostic indicators. No associations were found between survival and tumor location or the CBTC morphologic classification.[8]

ACKNOWLEDGMENT

This work was supported by a grant from the University of Glasgow, Small Animal Hospital Fund.

CONFLICT OF INTEREST DECLARATION

Authors declare no conflict of interest.

OFF-LABEL ANTIMICROBIAL DECLARATION

Authors declare no off-label use of antimicrobials.

INSTITUTIONAL ANIMAL CARE AND USE COMMITTEE (IACUC) OR OTHER APPROVAL DECLARATION

Approved by the Research Ethics Committee of the School of Veterinary Medicine of the University of Glasgow (Ref33a/17).

HUMAN ETHICS APPROVAL DECLARATION

Authors declare human ethics approval was not needed for this study.

ORCID

Roberto José-López https://orcid.org/0000-0002-0661-5562
Rodrigo Gutierrez-Quintana https://orcid.org/0000-0002-3570-2542
Sonia Añor https://orcid.org/0000-0002-1099-7698

REFERENCES

1. McGrath JT. Intracranial pathology in the dog. *Acta Neuropathol*. 1962;1 (Suppl I):3-4.

2. Dorn CR, Taylor DO, Frye FL, et al. Survey of animal neoplasms in Alameda and Contra Costa counties, California. Methodology and description of cases. *J Natl Cancer Inst*. 1968;40:295-305.
3. Song RB, Vite CH, Bradle CW, et al. Postmortem evaluation of 435 cases of intracranial neoplasia in dogs and relationship of neoplasm with breed, age and body weight. *J Vet Intern Med*. 2013;27:1143-1152.
4. Bagley RS, Gavin PR, Moore MP, et al. Clinical signs associated with brain tumors in dogs: 97 cases (1992-1997). *J Am Vet Med Assoc*. 1999;215:818-819.
5. Snyder JM, Shofer FS, Van Winkle TJ, et al. Canine intracranial primary neoplasia: 173 cases (1986-2003). *J Vet Intern Med*. 2008;22:172-177.
6. Chen L, Zhang Y, Yang J, et al. Vertebrate animal models of glioma: understanding the mechanisms and developing new therapies. *Biochim Biophys Acta*. 1836;2013:158-165.
7. Bentley RT, Ahmed AU, Yanke AB, et al. Dogs are man's best friend: in sickness and in health. *Neuro Oncol*. 2017;19(3):312-322.
8. Koehler JW, Miller AD, Miller CR, et al. A revised diagnostic classification of canine glioma: towards validation of the canine glioma patient as a naturally occurring preclinical model for human glioma. *J Neuropathol Exp Neurol*. 2018;77(11):1039-1054.
9. Hayes HM, Priester WA Jr, Pendergrass TW. Occurrence of nervous-tissue tumors in cattle, horses, cats and dogs. *Int J Cancer*. 1975;15:39-47.
10. Truvé K, Dickinson P, Xiong A, et al. Utilizing the dog genome in the search for novel candidate genes involved in glioma development–genome wide association mapping followed by targeted massive parallel sequencing identifies a strongly associated locus. *PLoS Genet*. 2016;12(5):e1006000.
11. Kraft SL, Gavin PR, DeHaan C, et al. Retrospective review of 50 canine intracranial tumors evaluated by magnetic resonance imaging. *J Vet Intern Med*. 1997;11:218-225.
12. Ródenas S, Pumarola M, Gaitero L, et al. Magnetic resonance imaging findings in 40 dogs with histologically confirmed intracranial tumours. *Vet J*. 2011;187:85-91.
13. Young BD, Levine JM, Porter BF, et al. Magnetic resonance imaging features of intracranial astrocytomas and oligodendrogliomas in dogs. *Vet Radiol Ultrasound*. 2011;52:132-141.
14. Bentley RT, Ober CP, Anderson KL, et al. Canine intracranial gliomas: relationship between magnetic resonance imaging criteria and tumor type and grade. *Vet J*. 2013;198(2):463-471.
15. Stadler KL, Ruth JD, Pancotto TE, et al. Computed tomography and magnetic resonance imaging are equivalent in mensuration and similarly inaccurate in grade and type predictability of canine intracranial gliomas. *Front Vet Scie*. 2017;4:157.
16. Louis DN, Ohgaki H, Wiestler OD, et al. The 2007 WHO classification of tumours of the central nervous system. *Acta Neuropathol*. 2007;114:97-109.
17. Higgins RJ, Bollen AW, Dickinson PJ, et al. Tumors of the nervous system. In: Meuten DJ, ed. *Tumors in Domestic Animals*. 5th ed. Arnes, AI: Willey-Blackwell; 2016:834-891.
18. Dickinson PJ. Advances in diagnostic and treatment modalities for intracranial tumors. *J Vet Intern Med*. 2014;28:1165-1185.
19. Louis DN, Ohgaki H, Wiestler OD, et al. The 2016 World Health Organization classification of tumors of the central nervous system: a summary. *Acta Neuropathol*. 2016;131:803-820.
20. Fernández F, Deviers A, Dally C, et al. Presence of neural progenitors in spontaneous canine gliomas: a histopathological and immunohistochemical study of 20 cases. *Vet J*. 2016;209:125-132.
21. Recio A, de la Fuente C, Pumarola M, et al. Magnetic resonance imaging and computed tomographic characteristics of a glioma causing calvarial erosion in a dog. *Vet Radiol Ultrasound*. 2019;60:E1-E5.
22. Lobacz MA, Serra F, Hammond G, et al. Imaging diagnosis – magnetic resonance imaging of diffuse leptomeningeal oligodendrogliomatosis in a dog with "dural tail sign". *Vet Radiol Ultrasound*. 2018;59:E1-E6.
23. Zagzag D, Esencay M, Mendez O, et al. Hypoxia- and vascular endothelial growth factor-induced stromal cell-derived factor-1α/CXCR4 expression in glioblastomas: one plausible explanation of Scherer's structures. *Am J Pathol*. 2008;173:545-560.
24. Rossmeisl JH, Clapp K, Pancotto TE, et al. Canine butterfly glioblastomas: a neuroradiological review. *Front Vet Sci*. 2016;3:40.
25. Schweizer-Gorgas D, Henke D, Oevermann A, et al. Magnetic resonance imaging features of canine gliomatosis cerebri. *Vet Radiol Ultrasound*. 2018;59:180-187.
26. Vigeral M, Bentley RT, Rancilio NJ, et al. Imaging diagnosis – antemortem detection of oligodendroglioma "cerebrospinal fluid drop metastases" in a dog by serial magnetic resonance imaging. *Vet Radiol Ultrasound*. 2018;59:E32-E37.
27. Koch MW, Sánchez MD, Long S. Multifocal oligodendroglioma in three dogs. *J Am Anim Hosp Assoc*. 2011;47:e77-e85.
28. Schkeeper AE, Moon R, Shrader S, et al. Imaging diagnosis – magnetic resonance imaging features of a multifocal oligodendroglioma in the spinal cord and brain of a dog. *Vet Radiol Ultrasound*. 2017;58:E49-E54.
29. Canal S, Bernardini M, Pavone S, et al. Primary diffuse leptomeningeal gliomatosis in 2 dogs. *Can Vet J*. 2013;54:1075-1079.
30. Ostrom QT, Cioffi G, Gittleman H, et al. CBTRUS statistical report: primary brain and other central nervous system tumors diagnosed in the United States in 2012-2016. *Neuro Oncol*. 2019;21(S5):v1-v100.
31. Sturges BK, Dickinson PJ, Bollen AW, et al. Magnetic resonance imaging and histological classification of intracranial meningiomas in 112 dogs. *J Vet Intern Med*. 2008;22:586-595.
32. Bittermann S, Lang J, Henke D, et al. Magnetic resonance imaging signs of presumed elevated intracranial pressure in dogs. *Vet J*. 2014;201:101-108.
33. Toyoda I, Vernau W, Sturges BK, et al. Clinicopathological characteristics of histiocytic sarcoma affecting the central nervous system in dogs. *J Vet Intern Med*. 2020;34:828-837.
34. Parker HG, Dreger DL, Rimbault M, et al. Genomic analyses reveal the influence of geographic origin, migration, and hybridization on modern dog breed development. *Cell Rep*. 2017;19:697-708.
35. Wood A, Garosi L, Platt S. Cerebrospinal fluid analysis. In: Platt S, Garosi L, eds. *Small Animal Neurological Emergencies*. London, UK: Manson Publishing; 2012:121-136.
36. Higgins RJ, Dickinson PJ, LeCouteur RA, et al. Spontaneous canine gliomas; overexpression of EGFR, PDGFRalpha, and IGFBP2 demonstrated by tissue microarray immunophenotyping. *J Neurooncol*. 2010;98:49-55.
37. Rissi DR, Levine JM, Eden KB, et al. Cerebral oligodendroglioma mimicking intraventricular neoplasia in three dogs. *J Vet Diagn Invest*. 2015;27:396-400.
38. Schwartz M, Lamb CR, Brodbelt DC, et al. Canine intracranial neoplasia: clinical risk factors for development of epileptic seizures. *J Small Anim Pract*. 2011;52:632-637.
39. Vecht CJ, Kerkhof M, Duran-Pena A. Seizure prognosis in brain tumors: new insights and evidence-based management. *Oncologist*. 2014;19:751-759.
40. Wolff CA, Holmes SP, Young BD, et al. Magnetic resonance imaging for the differentiation of neoplastic, inflammatory, and cerebrovascular brain disease in dogs. *J Vet Intern Med*. 2012;26:589-597.
41. Khalid L, Carone M, Dumrongpisutikul N, et al. Imaging characteristics of oligodendrogliomas that predict grade. *AJNR Am J Neuroradiol*. 2012;33:852-857.
42. Walker C, Baborie A, Crooks D, et al. Biology, genetics and imaging of glial cell tumors. *Br J Radiol*. 2011;84:S90-S106.
43. Watanabe M, Tanaka R, Takeda N. Magnetic resonance imaging and histopathology of cerebral gliomas. *Neuroradiology*. 1992;34:463-469.
44. Knopp EA, Cha S, Johnson G, et al. Glial neoplasms: dynamic contrast-enhanced T2*-weighted MR imaging. *Radiology*. 1999;211:791-798.

45. Reiche W, Grunwald I, Hermann K, et al. Oligodendrogliomas. *Acta Radiol*. 2002;43:474-482.
46. Walker C, du Plessis DG, Fildes D, et al. Correlation of molecular genetics with molecular and morphological imaging in gliomas with an oligodendroglial component. *Clin Cancer Res*. 2004;10:7182-7191.
47. Jenkinson MD, du Plessis DG, Smith TS, et al. Histological growth patterns and genotype in oligodendroglial tumors: correlation with MRI features. *Brain*. 2006;129:1884-1891.
48. Van den Bent MJ, Reni M, Gatta G, et al. Oligodendroglioma. *Crit Rev Oncol Hematol*. 2008;66:262-272.
49. Ginsberg LE, Fuller GN, Hashmi M, et al. The significance of lack of MR contrast enhancement of supratentorial brain tumors in adults: histopathological evaluation of a series. *Surg Neurol*. 1998;49:436-440.
50. Lee YY, Tassel PV. Intracranial oligodendrogliomas: imaging findings in 35 untreated cases. *AJR Am J Roentgenol*. 1989;152:361-369.
51. Engelhard HH, Stelea A, Mundt A. Oligodengroglioma and anaplastic oligodendroglioma: clinical features, treatment, and prognosis. *Surg Neurol*. 2003;60:443-456.
52. Matsukado Y, MacCarty CS, Kernohan JW. The growth of glioblastoma multiforme (astrocytomas, grades 3 and 4) in neurosurgical practice. *J Neurosurg*. 1961;18:636-644.
53. Rees JH, Smirniotopoulos JG, Jones RV, et al. Glioblastoma multiforme: radiologic-pathologic correlation. *Radiographics*. 1996;16:1413-1438.
54. Hardian RF, Goto T, Kuwabara H, et al. An autopsy case of widespread brain dissemination of glioblastoma unnoticed by magnetic resonance imaging after treatment with bevacizumab. *Surg Neurol Int*. 2019;10:137.
55. Walmsley GL, Chandler K, Davies ES, et al. Muti-focal cerebral oligoastrocytoma in a puppy. *J Small Anim Pract*. 2009;50:435-439.
56. Barnard RO, Geddes JF. The incidence of multifocal cerebral gliomas. A histologic study of large hemisphere sections. *Cancer*. 1987;60:1519-1531.
57. Ahn MS, Jackler RK. Exophytic brain tumors mimicking primary lesions of the cerebellopontine angle. *Laryngoscope*. 1997;107:466-471.
58. Wu B, Liu W, Zhu H, et al. Primary glioblastoma of the cerebellopontine angle in adults. *J Neurosurg*. 2011;114:1288-1293.
59. Kawakami S, Ochiai K, Azakami D, et al. R132 mutations in canine isocitrate dehydrogenase 1 (IDH1) lead to functional changes. *Vet Res Commun*. 2018;42:49-56.
60. Fraser AR, Bacci B, Chevoir MA, et al. Isocitrate dehydrogenase 1 expression in canine gliomas. *J Comp Pathol*. 2018;165:33-39.
61. Reitman ZJ, Olby NJ, Mariani CL, et al. IDH1 and IDH2 hotspot mutations are not found in canine glioma. *Int J Cancer*. 2010;127:245-246.
62. Amin SB, Anderson KJ, Boudreau CE, et al. Comparative molecular life history of spontaneous canine and human gliomas. *Cancer Cell*. 2020;37:243-257.e7.
63. Thomas R, Duke SE, Wang HJ, et al. 'Putting our heads together': insights into genomic conservation between human and canine intracranial tumors. *J Neurooncol*. 2009;94:333-349.
64. Rossmeisl JH Jr, Garcia PA, Pancotto TE, et al. Safety and feasibility of the NanoKnife system for irreversible electroporation ablative treatment of canine spontaneous intracranial gliomas. *J Neurosurg*. 2015;123:1008-1025.
65. Rossmeisl JH, Herpai D, Quigley M, et al. Phase I trial of convection-enhanced delivery of IL13RA2 and EPHA2 receptor targeted cytotoxins in dogs with spontaneous intracranial gliomas. *Neuro Oncol*. 2021;23(3):422-434. https://doi.org/10.1093/neuonc/noaa196.
66. Freeman AC, Platt SR, Holmes S, et al. Convection-enhanced delivery of cetuximab conjugated iron-oxide nanoparticles for treatment of spontaneous canine intracranial gliomas. *J Neurooncol*. 2018;137:653-663.
67. Bentley RT, Thomovsky SA, Miller MA, et al. Canine (pet dog) tumor microsurgery and intratumoral concentration and safety of metronomic chlorambucil for spontaneous glioma: a phase I clinical trial. *World Neurosurg*. 2018;116:e534-e542.
68. Suñol A, Mascort J, Font C, et al. Long-term follow-up of surgical resection alone for primary intracranial rostrotentorial tumors in dogs: 29 cases (2002-2013). *Open Vet J*. 2017;7:375-383.

SUPPORTING INFORMATION

Additional supporting information may be found online in the Supporting Information section at the end of this article.

How to cite this article: José-López R, Gutierrez-Quintana R, de la Fuente C, et al. Clinical features, diagnosis, and survival analysis of dogs with glioma. *J Vet Intern Med*. 2021;1–16. https://doi.org/10.1111/jvim.16199